ISSN 1070-3284, Russian Journal of Coordination Chemistry, 2018, Vol. 44, No. 3, pp. 173–178. © Pleiades Publishing, Ltd., 2018.

Multifunctional Gas Adsorption and Photocatalytic Degradation Based on a Porous Metal-Organic Framework Material[1]

E. H. Zhou[a, b], J. L. Jia[a], B. W. Wu[a], Z. D. Luo[c], J. Q. Liu[c], B. H. Li[c, *], and J. C. Jin[a, **]

[a]*Anhui Provincial Laboratory of Biomimetic Sensor and Detecting Technology, West Anhui University, Anhui, 237012 P.R. China*

[b]*West Anhui Health Vocational College, Anhui, 237012 P.R. China*

[c]*School of Pharmacy, Guangdong Medical University, Dongguan, 523808 P.R. China*

**e-mail: jcjgd2017@126.com*

***e-mail: gdmcli@126.com*

Received July 6, 2017

Abstract—The reaction of $Cu(NO_3)_2 \cdot 3H_2O$ with rigid ligand 4'-(1H-tetrazol-5-yl)-[1,1'-biphenyl]-3,5-dicarboxylic acid (H_3L) gave a new metal-organic framework of $[Cu_2(\mu_3\text{-}OH)(L)(H_2O)_2]_n$ (**I**) (CIF file CCDC no. 1533273). Complex **I** has a truncated cuboctahedra that was connected by trigonal $Cu_3O(N_4CR)_3$ trimers using each tetrazolate (N_4CR) moiety and shows a overall 3D nnt net with $(6.8^2)_6(8^3)_2(6^2.8^4)_3$ topology. The properties of gas adsorption and the degradation of the methyl violet have been examined.

Keywords: porous MOF, gas adsorption, photocatalysis property, topology

DOI: 10.1134/S1070328418030077

INTRODUCTION

Designed MOFs that are based on metal-organic polyhedra might provide very efficient ways for the construction of porous MOFs, because metal-organic polyhedra themselves have cavities, and the excellent properties of the MOFs could be modulated at the level of the metal-organic polyhedral [1]. Very common among the polyhedra is the cuboctahedron, which is often constructed with 12 dimetal paddle-wheel clustersand 24 isophthalate structural moieties [2, 3]. These polyhedra can be linked to form three-dimensional (3D) MOFs via either coordination bonds or covalent bonds, as demonstrated in [4–21]. Most recently, a (3,24)-connected network has been reported [22]; it was achieved by connecting the 24 edges of a cuboctahedron (or the 24 corners of a rhombicuboctahedron) with a linker having C_3 symmetry. Accordingly, from a pure topological analysis perspective, the rht-MOF can be alternatively described as a (3,3,4)-c net based on its basic building blocks (recently dubbed ntt). Recently, we have fabricated an uncommon (3,3,5)-c net by using a functionalized ligand strategy, which shows a high H_2 uptake exhibits a good selective adsorption of CO_2 over N_2 and CH_4 [23].

Following the supermolecular building blocks strategy, we selected and designed a new organic linker of 4'-(1H-tetrazol-5-yl)-[1,1'-biphenyl]-3,5-dicarboxylic acid (H_3L), which has more soft-base and hard-base coordination sites [24, 25]. It has ability to generate two types of binding moieties (carboxylate and pyrazole functionalities). Compared to common 5-tetrazolylisophthalic acid [8], it also contains larger size and easily forms pore feature when binds to metal centers. Herein, combining Cu^{2+} ions as the metal source and H_3L, we obtained a novel 3D porous MOF, $[Cu_2(\mu_3\text{-}OH)(L)(H_2O)_2]_n$ (**I**), constructed from the pyrazole-bridged cyclic trinuclear units. The properties of gas adsorption and the degradation of the methyl violet (MV) have been examined.

EXPERIMENTAL

Materials and methods. All chemicals were purchased from Jinan Henghua Sci. and Tec. Co. Ltd. without further purification. Powder X-ray diffraction (PXRD) data was collected on a Rigaku D/max-2550 diffractometer with CuK_α radiation (λ = 1.5418 Å). Elemental analyses (C, H, and N) were achieved by vario MICRO (Elementar, Germany). The thermogravimetric (TG) analyses were performed on TGA Q500 thermogravimetric analyzer used in air with a heating rate of 10°C min^{-1}.

Synthesis of I. Single crystal of **I** was obtained by solvothermal reaction of $Cu(NO_3)_2 \cdot 3H_2O$ (0.15 mmol) and H_3L (0.005 mmol) in DMF (2 mL) with HNO_3

[1] The article is published in the original.

Table 1. Crystallographic data and structure refinement information for **I**

Parameter	Value
Crystal system	Cubic
Crystal size	0.22 × 0.18 × 0.10
Space group	$Fm\bar{3}m$
Crystal color	Blue
V, Å ^{3}	161505(30)
Z	18
ρ_{calcd}, g/cm^3	0.450
μ	0.641
F(000)	21664
θ Range, deg	1.94–27.49
Index ranges	$-70 \le h \le 70$, $-70 \le k \le 58$, $-70 \le l \le 52$
Reflection collected	92646
Independent reflections (R_{int})	8677 (0.0354)
Numbers of paramrtes	615
GOOF	1.33
R_1, wR_2 ($I > 2\sigma(I)$)*	0.2946, 0.6488
R_1, wR_2 (all data)**	0.3672, 0.6014
$\Delta F_{max}/\Delta F_{min}$, e Å^{-3}	3.948/–1.543

* $R = \Sigma(F_o - F_c)/\Sigma(F_o)$, ** $wR_2 = \{\Sigma[w(F_o^2 - F_c^2)^2]/\Sigma(F_o^2)^2\}^{1/2}$.

(0.35 mL) (2.2 mL HNO_3 in 10 mL DMF) at 105°C for 72 h. The mixture was then cooled to room temperature. Bright-blue block crystals were obtained and air-dried (yield 35% based on Cu).

FT-IR (KBr; ν, cm^{-1}): 3350 w, 1623 m, 1582 s, 1456 m, 1358 s, 1240 m, 1104 w, 929 w, 880 w, 760 s, 721 m, 648 m.

The experimental PXRD pattern is in agreement with the simulated one based on the single crystal X-ray data, indicating the purity of the as-synthesized product.

X-ray structure determination. Crystallographic data for **I** was collected on a Bruker Apex II CCD diffractometer using graphite-monochromated MoK_α (λ = 0.71073 Å) radiation at 295 K. All nonhydrogen atoms were easily found from the difference Fourier map. The structure was solved by direct methods and refined by full-matrix least-squares on F^2 using version 5.1. All nonhydrogen atoms were refined anisotropically. Since the highly disordered guest molecules were trapped in the channels of **I** and could not be modeled properly, there are "Alert level A" about "Check Reported Molecular Weight" and "VERY LARGE Solvent Accessible VOID(S) in Structure" in the "check CIF/PLATON report" files for **I**. The final formula of **I** was derived from crystallographic data combined with elemental and TG analysis data. The detailed crystallographic data for **I** are listed in Table 1. Selected bond lengths and angles are listed in Table 2. The highly R vales may be assigned to its weak diffraction, which was caused by its larger cell and porous channel, although we have measured the data several times.

Crystallographic data for **I** have been deposited with Cambridge Crystallographic Data Centre (CCDC no. 1533273; www.ccdc.cam.ac.uk/data_request/cif).

Photocatalytic method. The photocatalytic reactions were performed as follows: 50 mg of **I** were dispersed in 50 mL aqueous solution of MV or RhB (10 mg/L) under stirring in the dark for 30 min to ensure the establishment of an adsorption–desorption equilibrium. Then the mixed solution was exposed to UV irradiation from an Hg lamp (250 W) and kept under continuous stirring during irradiation for 100 min. Samples of 5 mL were taken out every 10 min and collected by centrifugation for analysis by UV-Vis spectrometer. By contrast, the simple control experi-

Table 2. Selected bond distances (Å) and angles (deg) of structure **I***

Bond	*d*, Å	Bond	*d*, Å
Cu(1)–O(1)$^{\#1}$	1.970(7)	Cu(1)–O(4)	2.131(16)
Cu(1)–Cu(2)	2.663(3)	Cu(2)–O(2)$^{\#1}$	1.963(7)
Cu(2)–O(3)	2.190(14)	Cu(3)–O(12)	1.859(9)
Cu(3)–N(1)	1.911(17)		
Angle	ω, deg	Angle	ω, deg
O(1)Cu(1)O(1)$^{\#1}$	167.6(4)	O(1)Cu(1)O(4)	96.2(2)
O(1)Cu(1)Cu(2)	83.8(2)	O(2)Cu(2)O(2)$^{\#1}$	166.8(4)
O(2)Cu(2)O(3)	96.6(2)	O(12)Cu(3)N(1)	91.1(4)
N(1)Cu(3)N(1)$^{\#2}$	166.8(9)	Cu(3)O(12)Cu(3)$^{\#2}$	116.0(9)

* Symmetry codes: $^{\#1}$ $1-x, y, z$; $^{\#2}$ $1-x, 1-y, z$.

ment was also performed under the same condition without adding any catalysts.

The nitrogen adsorption–desorption measurements were carried out at liquid nitrogen temperature (77 K) by using an automatic volumetric adsorption equipment (Micromeritics, ASAP2020). Low pressure (<800 torr) gas sorption isotherms were performed using a Micromeritics ASAP 2020 surface area and pore size analyzer. Pore size distribution data were obtained from the N_2 sorption isotherms based on the DFT model in the Micromeritics ASAP 2020 software package (assuming slit pore geometry). An ultra-high purity (UHP, 99.999% purity) grade of N_2, H_2, CH_4, and CO_2 gases was used throughout the adsorption experiments. Prior to the measurements, all the samples were degassed at 80°C for 10 h to remove the adsorbed impurities.

RESULTS AND DISCUSSIONS

The structure of **I** contains L ligands coordinated to two types of copper cluster secondary building units (SBUs). The ligands, all of which are related by symmetry, coordinate to $Cu_3(OH)(Tz)_3$ clusters via the tetrazole functional group; each $Cu_3(OH)(Tz)_3$ SBU coordinates to three ligands in this way. Each ligand also coordinates via its carboxylate groups to two different (but symmetry related) copper carboxylate dimer SBUs. In other words, each inorganic paddlewheel unitis dinuclear and consists of two copper ions with a square pyramidal geometry, directing by four oxygen atoms of four carboxylates and one axial water molecule, CuO_5 (Fig. 1a). Both carboxylate moieties of the triply deprotonated L ligand coordinate in a bidentate bridging fashion to two copper atoms to form the $Cu_2(O_2CR)_4$ subunit, which combine in a *cis* fashion to form the finite truncated cuboctahedron. Each tetrazolate moiety also coordinates to two copper atoms of the $Cu_3O(N_4CR)_3$ trimer (Fig. 1b). It was very similar with the structure of $[Cu_6O(TZI)_3(H_2O)_9(NO_3)]_n \cdot (H_2O)_{15}$ (TZI = 5-tetrazolylisophthalicacid) [26].

From the topology view, complex **I** can also be interpreted topologically as a novel three-dimensional (3,3,4)-C connected ternary net, based on the assembly of three different basic SBUs. The ligand acts as a 3-c node, coordinating to two $Cu_2(O_2CR)_4$ and one $Cu_3(OH)(Tz)_3$ SBUs. In turn, the $Cu_2(O_2CR)_4$ SBU acts as a 4-c node and the $Cu_3(OH)(Tz)_3$ SBU acts as a 3-c node. This generates an overall 3D nnt net, which is a 3,3,4-c net with $(6.8^2)_6(8^3)_2(6^2.8^4)_3$ topology, as shown in Fig. 1b.

The permanent porosity of **I** was confirmed by the nitrogen adsorption studies at 77 K (Fig. 2a). The nitrogen adsorption of **I** exhibits a reversible isotherm and reaches saturation at 69.2 $cm^3 g^{-1}$ at 1 bar, indicating the microporous nature of the sample. Meanwhile, we also study its gas uptake capacity, especially for hydrogen, carbon dioxide and methane. We investigated the gravimetric H_2 uptake in **I** at 77 and 87 K (Figs. 2b, 2c). Both the H_2 isotherms show good reversibility without hysteresis, indicating that the interaction is physisorption. The H_2 uptake capacity reaches 85.03 $cm^3 g^{-1}$ at 77 K and 1.0 bar, and 64.8 $cm^3 g^{-1}$ at 87 K and 1.0 bar, respectively. Its value of H_2 capacity is less than that of

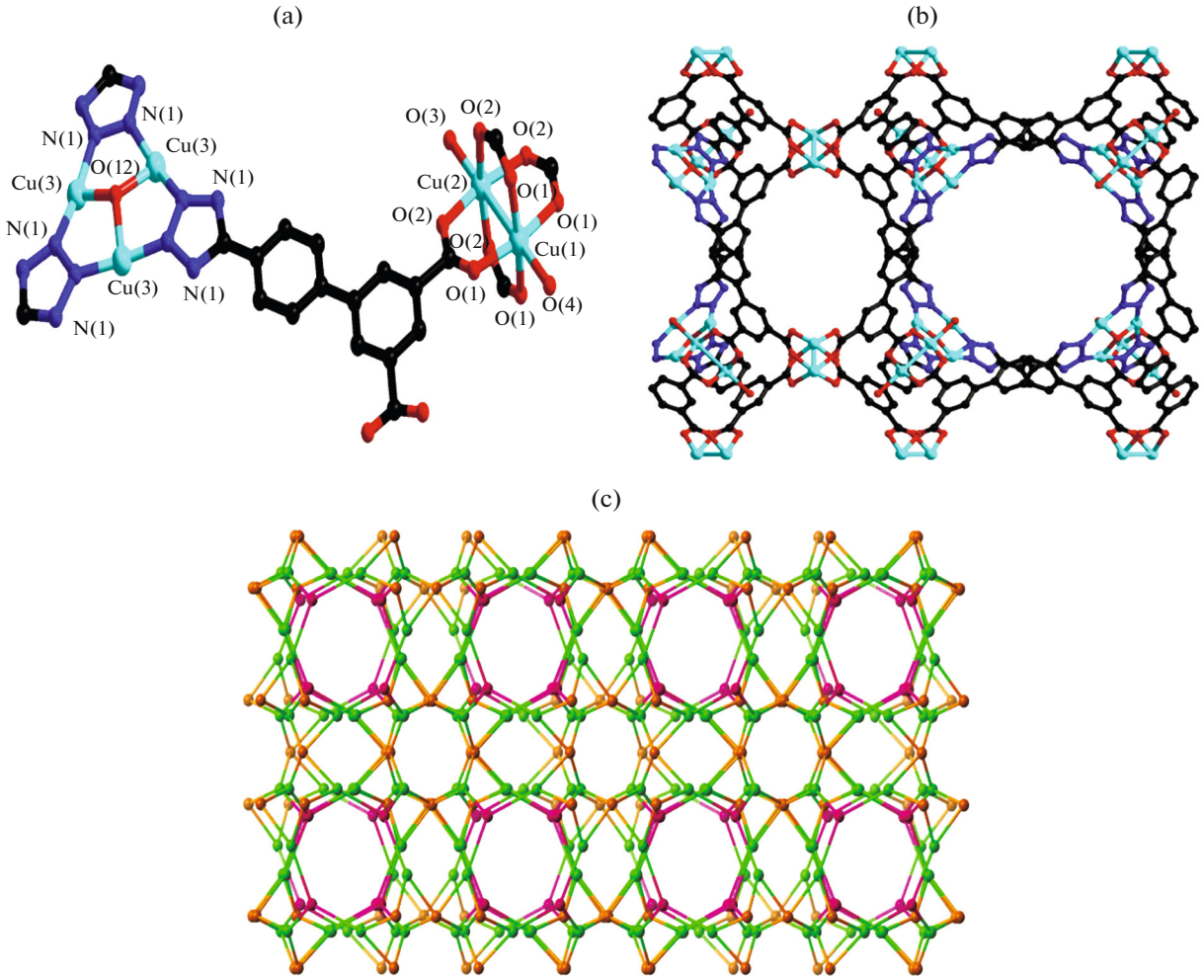

Fig. 1. View of the coordination environments of metal centers (a); the full 3D network with pore (b); and the underlying 3,3,4-c nnt net in the structure of **I** (c).

$[Cu_6O(TZI)_3(H_2O)_9(NO_3)]_n \cdot (H_2O)_{15}$ [26]. Besides, single component low pressure gas adsorption of CO_2 and CH_4 were also measured at 295 K (Figs. 2d, 2e), the maximum adsorbed amount of CO_2 and CH_4 on **I** is up to 27.4, 7.8 $cm^3\ g^{-1}$ at 295 K and 1 bar, respectively. From the lower gas uptake capacity, we found that the crystallized integrity was broken, which can be confirmed by PXRD patterns. Thus, the larger pore in this MOF is especially damaging for the gas uptake capacity. This phenomenon was also found in most reported MOFs [27, 28].

Based on the above structural feature, we tried to explore the photocatalytic activities of **I**. As shown in Fig. 3a, the absorption peaks of MV decrease obviously with the increasing of reaction time in the presence of **I**. The calculation results show that the degradation rate of MV is 64.2%. In addition, the control experiments on the degradation of organic pollutants were examined in the same reaction condition just without catalyst. The degradation rate of MV is just 17.8% within 100 min under UV irradiation without catalyst. The repeated photocatalytic degradation of a constant MV concentration was discussed. The degradation rates of **I** showed no significant reduction when the photocatalysts were used five times in the same procedures (Fig. 3b), which suggests that the photocatalytic activities have well reproducibility. After photocatalysis, the PXRD patterns of **I** has not more changed, implying that **I** maintains its structural interlinkage after the photocatalysis reaction. Herein, these facts indicate that **I** demonstrates excellent catalytic activity for the photodegradation of MV dye in water [29, 30].

TG analysis for **I** shows a weight loss of 16.6% between 35 and 138°C, which corresponding to the loss of DMF and coordinated H_2O molecules (calcd. 16.2%). Upon further heating, a weight loss of 58.6% should correspond to the release of the organic L ligands, and then the collapse of the framework (calcd. 58.0%) (Fig. 4).

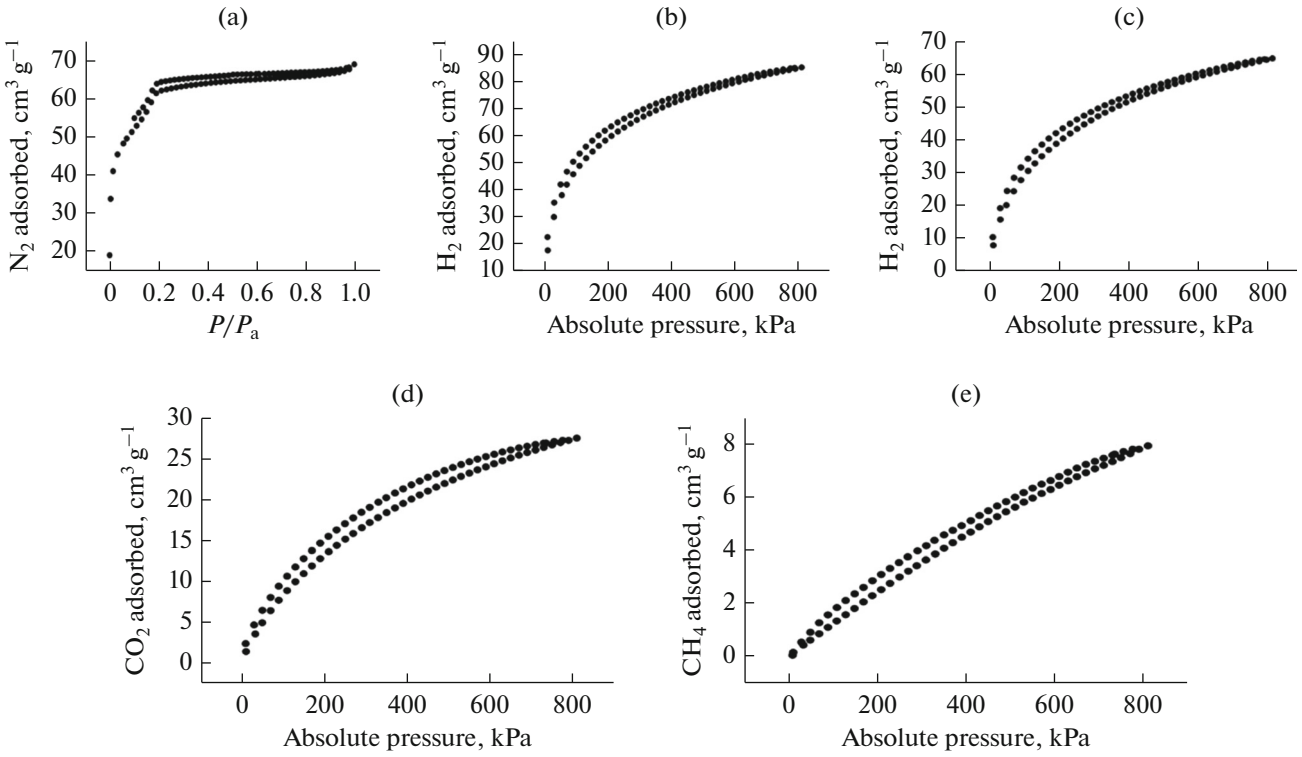

Fig. 2. N_2 adsorption isotherm of **I** at 77 K and 1 atm (a); H_2 adsorption isotherm of **I** at 77 and 87 K (b, c), respectively; CO_2, CH_4 adsorption isotherms at 295 K (d, e), respectively.

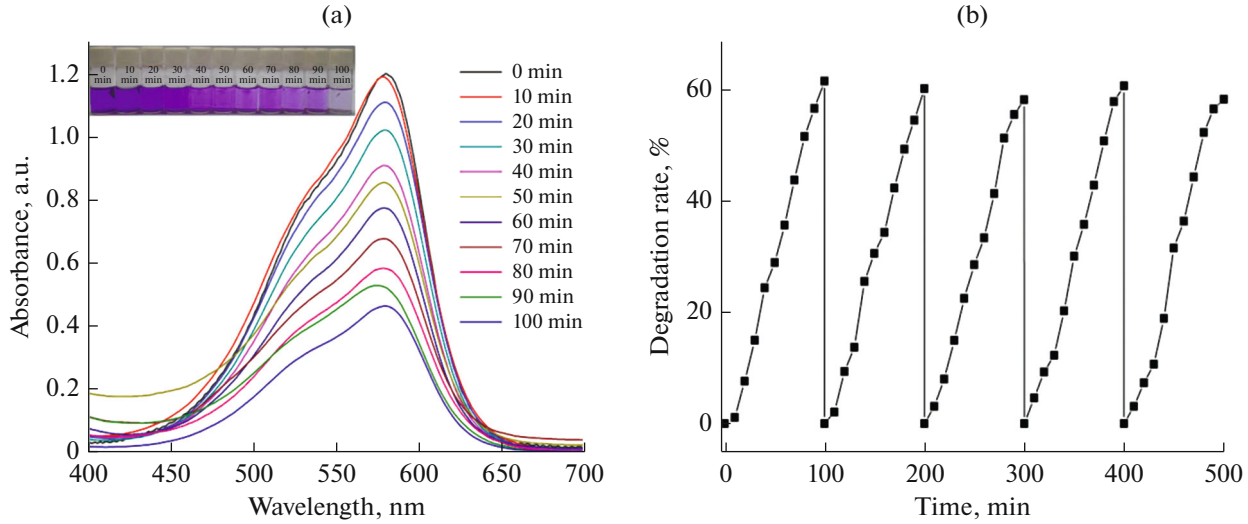

Fig. 3. UV-Vis absorption spectra of the MV solution during the decomposition reaction in the presence of **I** (a), recycling tests of **I** towards MV photodegradation (b).

In conclusion, a new 3D porous Cu(II) coordination polymers based on 4'-(1H-tetrazol-5-yl)-[1,1'-biphenyl]-3,5-dicarboxylic acid have been successfully synthesized and characterized. The results clearly indicated the higher pore in MOFs might be something that proves less helpful to the gas uptake capacity. In addition, **I** exhibits promising catalytic activities in the photodecomposition of the methyl violet dye.

ACKNOWLEDGMENTS

The authors acknowledge financial assistance from NSF of China (no. 21401143), and City Social

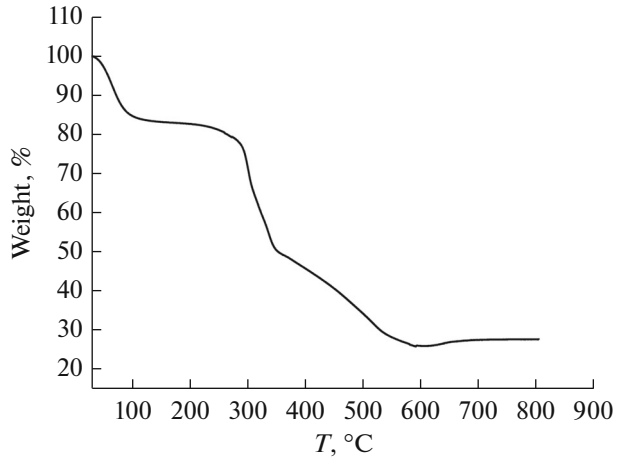

Fig. 4. TG curve for as-synthesized samples in **I**.

Science and Technology Development Program of Dongguan (grant 2016108101005) and Science Foundation funded project of Guangdong Medical University (Z2016001 and M2016023). We also very thanks for Prof. S.R. Battern and Dr. W.J. Wang for the contribution on this work.

REFERENCES

1. Zou, Y., Park, M., Hong, S., and Lah, M.S., *Chem. Commun.*, 2008, p. 2340.
2. Yan, Y., Lin, X., Yang, S., et al., *Chem. Commun.*, 2009, p. 1025.
3. Zhao, D., Yuan, D., Sun, D., and Zhou, H., *J. Am. Chem. Soc.*, 2009, vol. 131, p. 9186.
4. Eddaoudi, M., Kim, J., Wachter, J.B., et al., *J. Am. Chem. Soc.*, 2001, vol. 123, p. 436.
5. Abourahma, H., Coleman, A.W., Moulton, B., *J. Chem. Commun.*, 2001, vol. 22, p. 2380.
6. Moulton, B., Lu, J.J., Mondal, A., and Zaworotko, M.J., *Chem. Commun.*, 2001, p. 863.
7. Ke, Y.X., Collins, D.J., and Zhou, H.C., *Inorg. Chem.*, 2005, vol. 44, p. 4154.
8. Ni, Z., Yassar, A., Antoun, T., and Yaghi, O.M., *J. Am. Chem. Soc.*, 2005, vol. 127, p. 12752.
9. Furukawa, H., Kim, J., Plass, K.E., and Yaghi, O.M., *J. Am. Chem. Soc.*, 2006, vol. 128, p. 8398.
10. Moulton, B. and Zaworotko, M.J., *Chem. Rev.*, 2001, vol. 101, p. 1629.
11. Seidel, S.R. and Stang, P.J., *Chem. Res.*, 2002, vol. 35, p. 972.
12. Fujita, M., Tominaga, M., Hori, A., and Therrien, B., *Acc. Chem. Res.*, 2005, vol. 38, p. 368.
13. Tranchemontagne, D.J., Ni, Z., O'Keeffe, M., and Yaghi, O.M., *Angew. Chem. Int. Ed.*, 2008, vol. 47, p. 5136.
14. Lu, J., Mondal, A., Moulton, B., and Zaworotko, M.J., *Angew. Chem., Int. Ed.*, 2001, vol. 40, p. 2113.
15. McManus, G.J., Wang, Z.Q., and Zaworotko, M.J., *Cryst. Growth Des.*, 2004, vol. 4, p. 11.
16. Perry, J.J., Kravtsov, V.C., McManus, G.J., and Zaworotko, M.J., *J. Am. Chem. Soc.*, 2007, vol. 129, p. 10076.
17. Cairns, A.J., Perman, J.A., Wojtas, L., et al., *J. Am. Chem. Soc.*, 2008, vol. 130, p. 1560.
18. Nouar, F., Eubank, J.F., Bousquet, T., et al., *J. Am. Chem. Soc.*, 2008, vol. 130, p. 1833.
19. Chun, H.J., *J. Am. Chem. Soc.*, 2008, vol. 130, p. 800.
20. Wang, X.S., Ma, S.Q., Forster, P.M., *Angew. Chem., Int. Ed.*, 2008, vol. 47, p. 7263.
21. Yan, Y., Lin, X., Yang, S.H., et al., *Chem. Commun.*, 2009, p. 1025.
22. Perry, J.J., Perman, J.A., and Zaworotko, M.J., *Chem. Soc. Rev.*, 2009, vol. 38, p. 1400.
23. Liu, J., Liu, G., Gu, C., et al., *J. Mater. Chem., A*, 2016, vol. 4, p. 11630.
24. Hu, Y., Ding, M., Liu, X.Q., et al., *Chem. Commun.*, 2016, vol. 52, p. 5734.
25. Su, S., Zhang, Y., Zhu, M., et al., *Chem. Commun.*, 2012, vol. 48, p. 11118.
26. Nouar, F., Eubank, J.F., Bousquet, T., et al., *J. Am. Chem. Soc.*, 2008, vol. 130, p. 1833.
27. Babarao, R., Eddaoudi,M., and Jiang, J.W., *Langmuir*, 2010, vol. 26, p. 11196.
28. Ding, L. and Yazaydin, A.O., *Micro. Meso. Mater.*, 2013, vol. 182, p. 185.
29. Wu, Z.L., Wang, C.H., Zhao, B., et al., *Angew. Chem. Int. Ed.*, 2016, vol. 54, p. 4938.
30. Hu, J., Guo, R., Liu, Y., and Cui, G., *Inorg. Chim. Acta*, 2016, vol. 450, p. 418.